THE JOURNAL OF PHYSICAL CHEMISTRY B

Article

pubs.acs.org/JPCB

Direct Observation and Control of Ultrafast Photoinduced Twisted Intramolecular Charge Transfer (TICT) in Triphenyl-Methane Dyes

Guifeng Li, Donny Magana, and R. Brian Dyer*

Department of Chemistry, Emory University, Atlanta, Georgia, 30322, United States

Supporting Information

ABSTRACT: Femtosecond time-resolved infrared spectroscopy was employed to study intramolecular charge transfer in triphenylmethane dyes, including malachite green (MG), malachite green carbinol base (MGCB), and leucomalachite green (LMG). A local excited state (LE) and a twisted intramolecular charge-transfer (TICT) state have been observed directly in MG. Furthermore, solvent-controlled TICT measurements in a series of linear alcohols indicate that the transition time (4−11 ps) from LE to TICT is strongly dependent on alcohol viscosity, which is due to rotational hindrance of dimethylaniline in high-viscosity solvents. For LMG, no TICT is observed due to steric hindrance caused by the sp^3-hybridized central carbon atom. However, for MGCB, TICT is rescued by the addition of the electron-donating hydroxyl group to the bridge. These results for MG and its analogues provide new insight regarding the dynamics and mechanism of twisted intramolecular charge transfer (TICT) in triphenylmethane dyes.

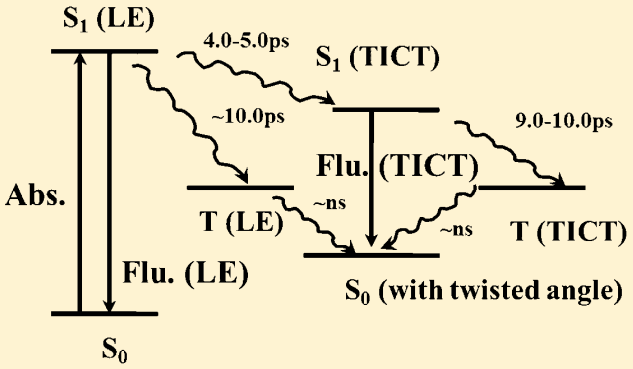

INTRODUCTION

Twisted intramolecular charge transfer (TICT) is a photoinduced charge separation process of fundamental and practical significance. TICT has been demonstrated in a number of organic dyes and used in a range of applications, including fluorescent probes, laser dyes, bistable switches, and molecular rotors.[1−4] Recent interest has focused on TICT as a possible mechanism for the ultrafast relaxation dynamics of excited states.[5] A model TICT system, 4-*N*,*N*-dimethylaminobenzonitrile (DMABN), exhibits dual fluorescence in polar solvents consisting of normal "B band" fluorescence (~350 nm, planar conformation, "local excited" LE state) and anomalous "A band" fluorescence (~450 nm, perpendicular conformation, TICT state), due to rotation of the dimethylamino (DMA) donor group.[6−8] TICT persists in systems where the nitrile group is substituted by other acceptors, such as naphthalene, anthracene, and other aromatic analogues. In these cases, the TICT mechanism involves rotation of the entire *N*,*N*-dimethylaniline unit instead of the DMA alone, confirmed by locking the system against rotation with a bridge structure.[7−10] Additional insight into the TICT mechanism has been provided by time-resolved infrared spectroscopy of the simple model system DMABN.[11−14]

TICT may also occur in more complex systems, such as malachite green (MG, Figure 1), a member of an important class of triphenylmethane (TPM) dyes with a wide range of applications.[2,15] MG has attracted attention due to its optical properties, including high extinction coefficient, viscosity-dependent fluorescence, and ultrafast nonradiative internal conversion.[2,16,17] Although the excited-state properties of MG have been investigated using electronic spectroscopy,[18−20] the role of TICT in the ultrafast relaxation dynamics of MG remains unclear.[21,22] Because rotation of dimethylaniline is involved in the TICT process, viscosity-dependent transient absorption and fluorescence up-conversion measurements have been carried out to probe the excited-state dynamics of MG.[21,23−26] Key observations from these studies include the following: (1) Ultrafast recovery of the ground state appears to be nonexponential and strongly depends on the viscosity of the solvent, which suggests involvement of an intermediate state produced by torsional motion of dimethylaniline,[25] and (2) results for dimethylmethano-bridged derivatives of MG demonstrate that fluorescence quenching of MG is related to

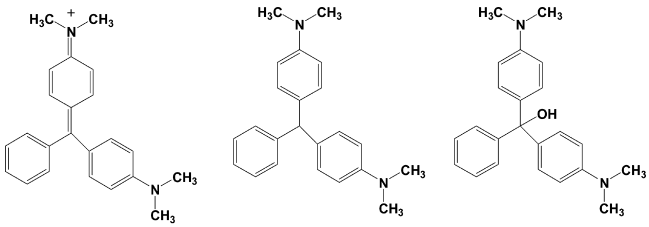

Figure 1. Chemical structures of (a) malachite green (MG), (b) leucomalachite green (LMG), and (c) malachite green carbinol base (MGCB).

Received: July 17, 2012
Revised: August 23, 2012
Published: September 25, 2012

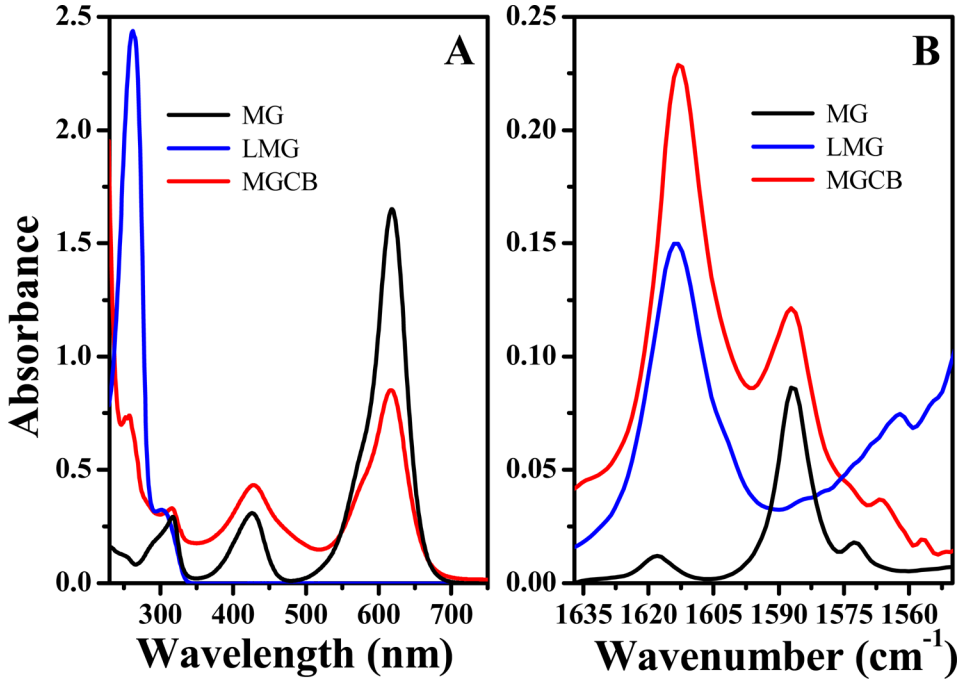

Figure 2. UV−vis (A) and FTIR (B) spectra of 1 mM MG (black), 15 mM LMG (blue), and 20 mM MGCB (red) in methanol.

twisting of the dimethylaniline.[21] A recent theoretical paper attempts to elucidate the ultrafast nonradiative excited-state processes of MG using CASPT2/CASCF quantum chemical calculations.[5] These calculations indicate that the initial population of the S_1 excited state (LE state) does not involve ring motions, whereas the ES relaxation process involves a rotation of the phenyl rings to form a TICT state. In the TICT state, the system can readily access the conical intersection between the S_1 and S_0 states and thereby efficiently decay back to the ground state.[5] Although the calculations provide a plausible explanation for the ultrafast ES relaxation of MG, there is no direct experimental evidence supporting this mechanism.

Here, we apply femtosecond mid-infrared spectroscopy to investigate the ultrafast excited-state deactivation of MG in polar solvents and the role of the TICT state in this process. Vibrational spectroscopy provides a more direct measure of the excited-state structural changes associated with TICT. Ultrafast IR experiments along with the viscosity dependence of the ES dynamics provide direct support for twisted intramolecular charge transfer. Additional evidence for the TICT mechanism is provided by comparison with two MG analogues, leucomalachite green (LMG, Figure1b) and malachite green carbinol base (MGCB, Figure1c). TICT is absent in LMG due to reduction of the central bridge but is rescued in the case of MGCB by the addition of the electron-donating hydroxyl group to the bridge.

EXPERIMENTAL SECTION

Chemicals. Malachite green (MG, Alfa Aesar), malachite green carbinol base (MGCB, Sigma-Aldrich), and leucomalachite green (LMG, Sigma-Aldrich) were used as received, and their chemical structures are shown in Figure 1. Linear alcohols of varying chain lengths, including methanol (≥99.8%, CH_3OH), 1-propanol (≥99.5%, $CH_3(CH_2)_2OH$), 1-pentanol (≥99%, $CH_3(CH_2)_4OH$), and 1-heptanol (≥98%, $CH_3(CH_2)_6OH$), were used as received from Sigma-Aldrich for viscosity-dependent measurements. Phosphate buffer solution (50 mM, pH = 7.0) was prepared from potassium phosphate monobasic (KH_2PO_4, ACS reagent) and potassium phosphate dibasic (K_2HPO_4, ACS reagent) in a 1:1 ratio in D_2O (99.9% D, Cambridge Isotope Laboratories, Inc.). Potassium deuteroxide (KOD, 40 wt % solution in D_2O, 98+ atom % D) and deuterium chloride solution (35 wt % in D_2O, 99 atom % D) were used for pH adjustment of the buffer. The concentration of MG was 1 mM in different alcohols and buffer for UV−vis, FT-IR, and transient IR measurements. Higher concentrations of 15 mM LMG and 20 mM MGCB in methanol were used for all measurements of these analogues. Perdeuterated methanol (methanol-d_4, 99.8% D, Cambridge Isotope Laboratories, Inc.) was used to provide a clear spectral window for time-resolved infrared (TRIR) measurements of MG at low frequency (<1400 cm^{-1}).

Femtosecond Time-Resolved Infrared Measurements. Transient infrared absorption spectra were obtained using a femtosecond pump−probe technique. The details of the setup have been described recently.[27] Briefly, the TRIR experiments were carried out in the following way: 800 nm laser pulses (3.6 W, 1 kHz, 30 fs) were generated with a femtosecond Ti:sapphire regenerative amplifier (Legend Elite, Coherent) seeded by a femtosecond Ti:sapphire mode-locked oscillator (Mantis, Coherent). The regenerative amplifier output was split in a 1:1 ratio and sent into two OPA systems (OPerA Solo, Coherent) used to generate the UV/vis pump pulses and IR probe pulses, respectively. The pump wavelength was 560 or 300 nm (1 mW) generated from the second harmonic or fourth harmonic of the signal beam from the OPA. The transient IR signal was dispersed in a mid-IR spectrograph and detected by an ImagIR infrared camera (HgCdTe, 2−10 μm, 128 × 128 array, Santa Barbara Focalplane) using LabVIEW (National Instruments) control software.

The sample solution was flowed by a fluid metering RHSY lab pump (Scientific Support Inc.) through a demountable IR liquid flow cell with Swagelok fittings (DSC-S25, Harrick

dx.doi.org/10.1021/jp307091f | J. Phys. Chem. B 2012, 116, 12590−12596

Scientific Products Inc.). The path length was 80 μm (for MG measurements) or 250 μm (for MGCB and LMG), which was set by the Teflon spacer thickness between two polished circular CaF_2 windows (25 mm × 2 mm, Koch Crystal Finishing, Inc.).

FT-IR and UV/vis Measurements. FTIR and UV/vis measurements for MG/alcohol solutions were made in a CaF_2 cell with an 80 μm path length, whereas for MGCB and LMG, methanol solutions were held in an amalgamated sealed cell (McCarthy Scientific Co.) having a 250 μm Teflon spacer between two polished rectangular CaF_2 windows (38.5 mm × 19.5 mm × 4 mm, Koch Crystal Finishing, Inc.). Steady-state FTIR spectra were collected using a Varian 660 IR spectrometer with an average of 128−256 scans at a 2 cm^{-1} spectral resolution. Steady-state UV/vis spectra were collected using a Lambda35 spectrophotometer (PerkinElmer).

RESULTS AND DISCUSSION

Ground States of MG, LMG, and MGCB. The previously reported electronic spectrum of *N*,*N*-dimethylaminobenzonitrile (DMABN) shows only two peaks at 250 nm (S_2) and 300 nm (S_1) due to charge transfer from the nitrogen lone pair to the phenyl ring.[28,29] In MG and its derivatives (LMG and MGCB), the combination of two dimethylanilines and one phenyl ring tethered by a central carbon bridge produces more complex absorption spectra. Figure 2A shows the UV/vis spectra of 1 mM MG (black line), 15 mM LMG (blue line), and 20 mM MGCB (red line) in methanol. The UV/vis spectrum of MG contains three peaks at 312, 425, and 617 nm. The peaks at 425 and 617 nm are due to splitting of the excited state in the low symmetry of MG,[17] assigned as the S_2 and S_1 states, respectively.[30] The shoulder at 570 nm may come from an isomer of MG.[24] Reduction of MG and of the dimethylaniline converts MG into LMG. LMG exhibits a completely different UV/vis spectrum, as shown in Figure 2A (blue line): the two peaks at 425 and 617 nm disappear. The spectral profile of LMG is similar to that of DMABN, suggesting that the three substituents linked by the central carbon have little electronic interaction with one another. In contrast, when the electron-donating hydroxyl group is added to the central carbon bridge in MGCB, the spectral features of the MG UV/vis are recovered, as shown in Figure 2A (red line). The only difference is the lower absorption coefficient of the MGCB bands compared to that of MG.

In comparison with the UV−vis results, a more dramatic spectral change is observed in the FTIR spectra of MG and its analogues, as shown in Figure 2B. The peak at 1618 cm^{-1} in the FTIR spectrum of MG (black line) has been assigned to phenyl−N and C−C stretching, based on molecular orbital calculations combined with Raman spectra.[31] Two other prominent features at 1586 and 1572 cm^{-1} have been assigned to stretching modes of the benzene ring.[32,33] The IR peak from the phenyl−N stretch is at 1372 cm^{-1}, which is observed at 1368 cm^{-1} in the Raman spectrum. In alcohol solution, a solvent band interferes with the observation of this IR peak. In contrast to MG, a peak at 1613 cm^{-1} dominates the LMG IR spectrum (Figure 2B, blue line), which is also due to the phenyl−N and C−C stretching modes. The strong peak at 1586 cm^{-1} observed for MG decreases to a small peak in the LMG spectrum, because the C═N bond is reduced to a single bond in the latter case. The IR spectrum of MGCB (Figure 2B, red line) is intermediate between those of MG and LMG. When an electron-donating group (OH) is added to the central carbon bridge position, it induces the appearance of an IR peak at 1586 cm^{-1} again, but the intensity of this band is still weak in comparison with that of MG. The peak at 1613 cm^{-1} dominates the IR spectrum of MGCB, similar to the LMG case.

Excited States of MG, LMG, and MGCB. *TRIR Spectroscopy of MG.* Ultrafast IR spectroscopy enables the direct observation of the LE and TICT states of MG in methanol. The two peaks at 1586 and 1618 cm^{-1} in the IR spectrum of MG are ideal probes of excited-state charge-transfer dynamics. As discussed above, they are assigned to the in-plane ring stretch and phenyl−N stretch of the *N*,*N*-dimethylaniline group and, therefore, are very sensitive to the electron density on the dimethylaniline group. Figure 3A shows the excited-state IR spectra of 1 mM MG in methanol at various times after 560 nm excitation. The pure excited-state spectra are obtained by addition of the ground-state FTIR spectrum to the transient spectra obtained after photoexcitation, in order to remove the bleach of the ground-state bands (Figure S1, Supporting Information, shows the raw transient spectra before subtraction). Addition of 16% of the ground-state spectrum effectively cancels the bleach, consistent with the expected degree of GS depletion based on the excitation conditions. The resulting ES spectra clearly show three bands at 1580, 1575, and 1569 cm^{-1} with time-dependent intensities. The peak at 1580 cm^{-1} increases with time, with a concomitant decrease in the peak intensities at 1575 and 1569 cm^{-1}, indicating the evolution of the system from the initially populated excited state to an intermediate state. The evolution of the ES spectrum reveals the dynamics of the charge-transfer processes following initial excitation. The dominant IR band is split in two bands and shifted to lower frequency in the state formed immediately

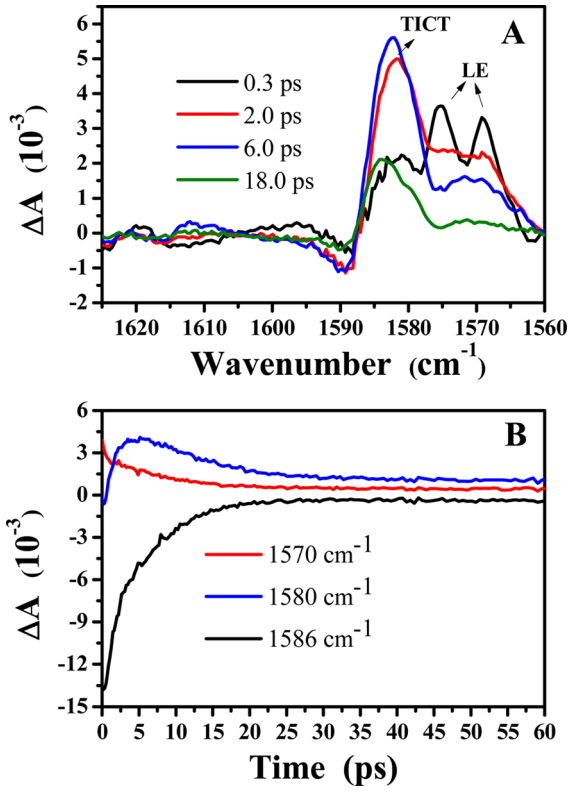

Figure 3. (A) Excited-state TRIR spectra and (B) IR transients of 1 mM MG in methanol following excitation at 560 nm.

dx.doi.org/10.1021/jp307091f | J. Phys. Chem. B 2012, 116, 12590−12596

after excitation. This splitting is clear evidence for a localized excitation (LE) on one of the two dimethylanilines, making them inequivalent and thus producing two bands. At later times, this initial state evolves to an intermediate state with symmetric dimethylanilines and thus only one broad peak (similar to the ground state) at 1580 cm^{-1}. The time-dependent evolution of the spectrum is consistent with CT to the phenyl group and localization of the hole on the central bridge C atom, making both the dimethylaniline groups equivalent again. The asymmetric charge distribution on the dimethylaniline rings is also evident in other vibrations, most prominently in the bending mode of the dimethylaniline ring methyl group at 1373 cm^{-1}, as shown in the Supporting Information (Figure S2). In the TRIR spectrum of the initial LE excited state (0.3 ps), this bending mode is split into two peaks at 1427 and 1410 cm^{-1} (Figure S3, Supporting Information), a clear indication of a localized excitation on one of the dimethylanilines. The split LE excited-state absorbance peaks collapse to a single absorbance at 1363 cm^{-1} within a few picoseconds, consistent with rapid relaxation to the TICT or triplet state with a symmetric charge distribution (Figure S3, Supporting Information).

Analysis of the IR transients obtained at different probe frequencies provides further insight regarding the excited-state dynamics. Figure 3B shows the IR transients probed at 1570, 1580, and 1586 cm^{-1}. The IR transient at 1580 cm^{-1} (TICT state) shows a rise time of 4.8 ± 0.5 ps and reaches its maximum intensity by 6.5 ps. This intermediate state then relaxes with a 10.5 ± 0.2 ps lifetime to a second intermediate state with a small amplitude and a long lifetime (likely a triplet state), producing an offset from zero that persists out to the longest times measurable in our experiment (>1 ns). The yield of the triplet state is 3% of the initial excited-state population. In contrast, the IR transient at 1570 cm^{-1} (LE state) rises instantaneously (~100 fs), then relaxes in two phases with lifetimes of 5.5 ± 0.3 and 10.0 ± 0.2 ps. The 5.5 ps phase corresponds to the decay to the TICT intermediate state, whereas the slower decay is due to the subsequent relaxation back to the ground state and to the triplet state. Again, the triplet state yield is very low based on the small, long-lived residual signal at 1570 cm^{-1}. The GS bleach signal at 1586 cm^{-1} shows an initial lag phase, followed by rapid recovery of most of the GS absorbance with a lifetime similar to the second exponential phase of the ES relaxation. A small residual signal is also observed for the GS bleach at long times, corresponding the long-lived triplet state.

A TICT model can be used to explain these results. The initial excited state that appears within the laser pulse, characterized by sharp IR bands at 1569 and 1575 cm^{-1}, is assigned to the LE state with an asymmetric charge distribution on the dimethylaniline rings. This state rapidly decays to the TICT state, having a single band at 1580 cm^{-1} analogous to the GS spectrum, but shifted to lower frequency. The rise time (4.8 ± 0.5 ps) of the 1580 cm^{-1} IR transient represents the transition time from the singlet LE state to the singlet TICT state. The 10.5 ± 0.2 ps process represents the decay of the singlet TICT state, either by return to the GS or by intersystem crossing to the triplet TICT state. The recovery of the GS bleach occurs on this same time scale, but the residual, long-lived (>1 ns) bleach and transient absorbances are consistent with a small fraction of the excited molecules undergoing ISC to the triplet TICT state.

Solvent Dependence of MG Excited-State Dynamics. The solvent dependence of the TRIR spectrum of MG was measured in order to test the model of charge transfer from a twisted conformation. Increasing the carbon chain length of the linear alcohol solvent increases the viscosity, which, in turn, progressively hinders the rotation of the dimethylaniline substituent. In addition, increasing the carbon chain length of the alcohol decreases the solvent polarity, which also inhibits the formation of the charge-separated state. Therefore, if the excited state of MG evolves through twisted charge transfer, it should be possible to control this process by systematically varying the solvent properties. Figure 4A shows the 6.0 ps

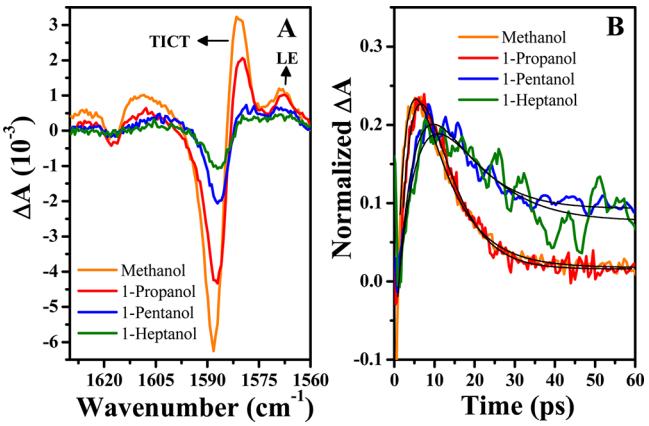

Figure 4. (A) TRIR spectra (6 ps) and (B) transient decays at 1579 cm^{-1} of 1 mM MG in methanol (black), 1-propanol (red), 1-pentanol (blue), and 1-heptanol (green) excited at 560 nm. Fits to a double-exponential function are plotted as red lines.

TRIR spectra of MG in a series of alcohols with chain lengths varying from one to seven carbons. Two negative peaks at 1586 and 1618 cm^{-1} are observed as ground-state bleaches, which are assigned to the phenyl ring and phenyl−N stretching vibrations. Two positive bands around 1581 and 1568 cm^{-1} are attributed to TICT and LE states, respectively. With increasing carbon chain length of the alcohol, the ground-state bleach at 1586 cm^{-1} shifts to lower frequency due to the decrease in polarity of the solvent. More importantly, the trend for the excited-state bands indicates a reduction in the yield of the TICT state (1581 cm^{-1} band) as the solvent viscosity is increased and the polarity is decreased. We emphasize that the spectra in Figure 4A are snapshots of the dynamics at 6.0 ps, and so the transition from LE to TICT states is nearly complete for methanol, but only just getting started for 1-heptanol. The IR transients monitored at 1581 cm^{-1} in different alcohols are shown in Figure 4B. The amplitudes of these transients have been scaled to the initial (300 fs) GS bleach at 1586 cm^{-1} so that each represents the initial yield of the LE state and subsequent TICT yield. The rise and decay profiles are characteristic of formation of the TICT state and its subsequent decay either to the triplet state or back to the ground state. The rise time of the 1581 cm^{-1} band is the time of conversion from the LE to the TICT state. This rise time increases with increasing chain length of the alcohol, from 4.2 ± 0.5 ps for methanol to 11.4 ± 0.4 ps for heptanol, as expected for inhibited twisting and charge transfer in the higher-viscosity and lower-polarity solvent (a summary of the dynamics of the TICT state of MG in different solvents is shown in the Supporting Information, Table S1). Therefore, the data are

dx.doi.org/10.1021/jp307091f | J. Phys. Chem. B 2012, 116, 12590−12596

consistent with the assignment of this process to TICT. A similar dependence of the TICT yield on solvent polarity has been observed for DMABN using ultrafast IR spectroscopy.[12,13]

The preceding analysis does not account for the decrease in solubility of MG (and, therefore, a decrease in overall IR signal levels) with an increase in the alcohol carbon chain length. The TICT yield can be evaluated more quantitatively by comparing the intensity of the ground-state bleach at 0.3 ps (which gives the yield of the initial LE state) to the TICT excited-state absorbance at longer times. Because the observed IR band widths do not depend on the 1-alkanol solvent, we define the TICT yield as the ratio of the maximum intensity of the excited-state TICT band (1581 cm^{-1}) to the initial ground-state bleach (1586 cm^{-1}) at 0.3 ps. It is important to note that the TICT excited-state spectrum overlaps the ground-state bleach (Figure 4A), so the initial GS bleach (at 0.3 ps, prior to formation of the TICT state) must be used to avoid interference from the TICT state. Figure 5 shows the TICT yield of MG in 1-alkanol plotted as a function of the solvent viscosity at 298 K.[34] The TICT yield decreases monotonically from a maximum of 0.24 for MG in methanol. These results are comparable to the viscosity-dependent TICT yield for crystal violet (CV) determined by transient visible absorbance methods.[35,36] A linear viscosity dependence has been observed for the excited-state absorbance, ground-state recovery lifetime, and radiationless relaxation lifetime of CV in relatively low-viscosity 1-alkanol solutions (carbon chain length < 5).[35,36] MG shows a similar linear dependence for the full viscosity range probed, as shown in Figure 5.

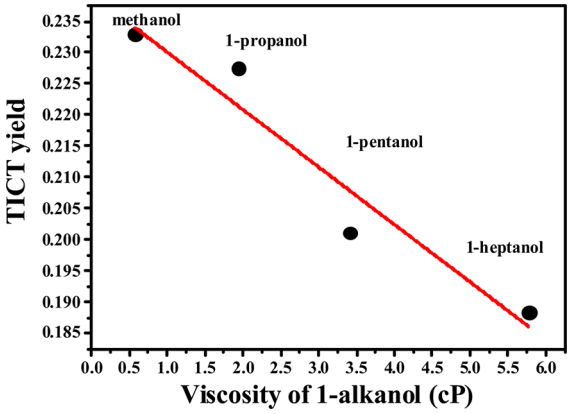

Figure 5. TICT yield as a function of 1-alkanol viscosity for MG solutions at room temperature.

TRIR Results for LMG in Methanol. Comparison of the ultrafast dynamics of MG with its analogues provides additional insight into the TICT mechanism. Reduction of MG produces the leuco structure (LMG, Figure 1b) that no longer absorbs in the visible due to loss of electronic coupling between the separate aromatic rings. Figure 6 shows the FTIR and TRIR spectra (A) and IR transients (B) for LMG. The TRIR spectrum of LMG has none of the features observed for the TICT state of MG, but rather is dominated by a long-lived bleach of the 1618 cm^{-1} band that persist for at least 1 ns (the limit of our optical delay line). The fluorescence lifetime of dimethylaniline in ethanol is 2.85 ns,[37] which suggests that the ES dynamics of LMG is similar to that of dimethylaniline. We conclude that the reduction of the bridge decouples the dimethylanilines from one another and from the phenyl group, inhibiting formation of the TICT state. Although the charge transfer from the excited state of dimethylaniline to the phenyl group is still energetically favorable, the presence of the saturated bridge prevents it. Steric hindrance of the sp^3-hybridized central carbon in LMG restricts rotation of dimethylaniline around the C−C bond. Because it is harder in this case for the system to access a perpendicular conformation between donor and acceptor, it never reaches the energetic minimum required for efficient TICT. We conclude that twisting of the double bond between the dimethylaniline and phenyl rings is a crucial part of the main deactivating event. This conclusion is supported by previous studies of the effect of the bridge between a dimethylaniline and phenyl group on fluorescence quenching. Rettig et al. observed strong fluorescence quenching attributed to TICT when the single bond connecting the two is converted to an ethylene group.[38] Fluorescence quenching is reduced when the double bond is included in a five-membered carbocyclic ring because rotation of dimethylaniline is restricted.[38]

TRIR Results for MGCB in Methanol. The TICT process can be rescued in the case of a saturated bridge by addition of an electron-donating group to the central bridge carbon atom, such as the OH group in MGCB (Figure 1c). Thus, for MGCB, we observe the same transient IR signatures of the LE and TICT states that we observe for MG, as shown in Figure 6C. The relaxation time from the initial LE state to the TICT state of MGCB is 4.8 ± 0.5 ps, as shown in Figure 6D, which is similar to that of MG. The most significant difference between the MG and the MGCB TRIR spectra is that the strong IR peak at 1613 cm^{-1} is almost absent in the case of MGCB. This observation suggests that the charge localization in the TICT excited state of MGCB is different from that of MG. Nevertheless, it is clear that TICT occurs in this case, despite the saturation of the bridge. Therefore, the OH group must play an important role in the TICT process, helping to bridge the electron transfer between the dimethylaniline and phenyl ring.

Summary of Excited-State Dynamics. The simple TICT diagram shown in Figure 7 summarizes our analysis of the ultrafast ES dynamics of MG in polar solvents. Photoexcitation populates the LE state (S_1), which quickly relaxes to a singlet TICT state within 4−11 ps, the rate of CT depending on solvent viscosity. The lifetime for intersystem crossing from the singlet to triplet LE states is about 8 ps based on the decay of the LE signature in the TRIR spectrum. Theory predicts that the triplet LE state decays to a twisted ground state S_0 (twisted) because the twisting process occurs before formation of the LE triplet.[5] The singlet TICT state relaxes with a lifetime of 10 ps back to the ground state in the predominant pathway (based on recovery of the GS bleach). Because this is the dominant pathway, the TICT process results in rapid and efficient deactivation of the excited state. A small fraction (3%) of the population undergoes intersystem crossing to the triplet TICT state. The triplet state likely decays by emission to a twisted ground state, accounting for the large Stokes shift in the anomalous fluorescence band.

■ CONCLUSIONS

We have successfully applied femtosecond time-resolved infrared (TRIR) spectroscopy to study charge transfer in MG and its analogues (LMG and MGCB) in polar solvents. The TRIR results provide new insight into the nature of the excited states produced. Initial excitation of MG or MGCB produces a

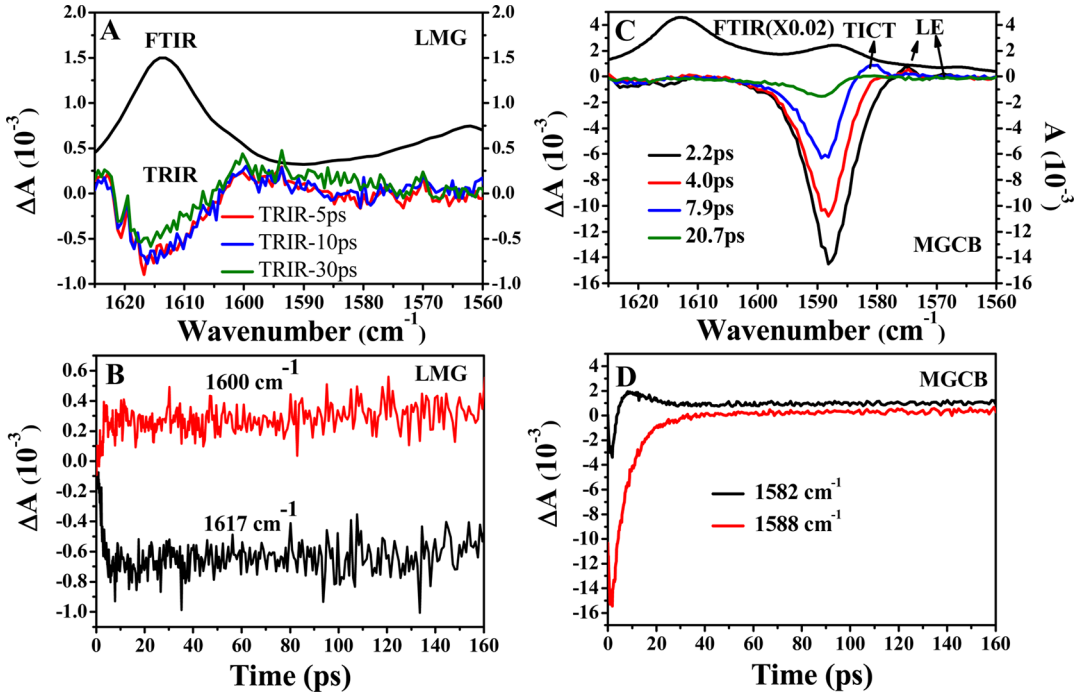

Figure 6. FTIR and TRIR spectra and IR transients of (A, B) 15 mM LMG (310 nm excitation) and of (C, D) 20 mM MGCB (560 nm excitation) in methanol.

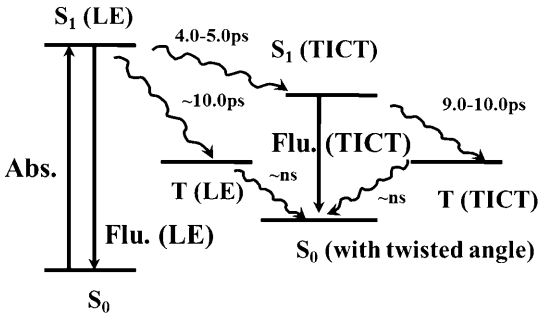

Figure 7. Proposed photophysical scheme of excited MG.

highly localized state LE, that has inequivalent dimethylaniline groups due to charge localization on one of the two dimethylanilines. Rapid relaxation of this state to the TICT state yields a more symmetric charge distribution, consistent with transfer of an electron to the phenyl group and the hole on the bridge carbon. The transition time from LE to TICT has a range of 4−11 ps, depending on the solvent viscosity. With an increase of solvent viscosity, the transition time from LE to TICT increases, whereas the relaxation time of the TICT singlet back to the ground state is about the same (10 ps), consistent with the hindered rotation of the dimethylaniline. Therefore, the dominant excited-state deactivation pathway in MG is through internal conversion of the TICT state to the ground state. In contrast, no TICT state is observed in LMG due to steric hindrance of the saturated bridge that restricts rotation of dimethylaniline relative to the phenyl ring. Introduction of an electron-donating group, OH, to the central carbon atom of the saturated bridge rescues the TICT process. Thus, for MGCB, we observe the IR signatures of the LE and TICT states. These results demonstrate that the OH group plays an important bridge role in the charge-transfer process, enabling efficient CT from the dimethylaniline to the phenyl ring.

■ ASSOCIATED CONTENT

Supporting Information

The Supporting Information contains supporting figures as indicated in the text. This material is available free of charge via the Internet at http://pubs.acs.org.

■ AUTHOR INFORMATION

Corresponding Author

*Phone: +1-404-727-6637. E-mail: briandyer@emory.edu.

Notes

The authors declare no competing financial interest.

■ ACKNOWLEDGMENTS

This work was supported by the NIH grant GM068036.

■ REFERENCES

(1) Haidekker, M. A.; Theodorakis, E. A. *J. Biol. Eng.* **2010**, *4*, 1−14.
(2) Rettig, W. In *Topics in Fluorescence Spectroscopy: Probe Design and Chemical Sensing*; Lakowicz, J. R., Ed.; Springer: New York, 1994; Vol. *4*.
(3) Haidekker, M. A.; Theodorakis, E. A. *Org. Biomol. Chem.* **2007**, *5*, 1669−1678.
(4) Rettig, W. *Appl. Phys. B: Lasers Opt.* **1988**, *45*, 145−149.
(5) Nakayama, A.; Taketsugu, T. *J. Phys. Chem. A* **2011**, *115*, 8808−8815.
(6) Lippert, E., Liider, W., Boos, H., Eds. *Advances in Molecular Spectroscopy*; Pergamon: Oxford, U.K., 1962.
(7) Rettig, W. In *Electron Transfer I: Photoinduced Charge Separation via Twisted Intramolecular Charge Transfer States*; Mattay, J., Eds.; Topics in Current Chemistry; Springer-Verlag: Berlin, 1994; Vol. *169*, pp 253−299.
(8) Rettig, W. *Angew. Chem., Int. Ed. Engl.* **1986**, *25*, 971−988.
(9) Siemiarczuk, A.; Grabowski, Z. R.; Krówczyński, A.; Asher, M.; Ottolenghi, M. *Chem. Phys. Lett.* **1977**, *51*, 315−320.

(10) Grabowski, Z. R.; Rotkiewicz, K.; Rettig, K. *Chem. Rev.* **2003**, *103*, 3899−4032.
(11) Kwok, W. M.; George, M. W.; Grills, D. C.; Ma, C. S.; Matousek, P.; Parker, A. W.; Phillips, D.; Toner, W. T.; Towrie, M. *Angew. Chem., Int. Ed. Engl.* **2003**, *46*, 1826−1830.
(12) Hashimoto, M.; Hamawchi, H. *J. Phys. Chem.* **1995**, *99*, 7875−7877.
(13) Kwok, W. M.; Ma, C.; George, M. W.; Grills, D. C.; Matousek, P.; Parker, A. W.; Phillips, D.; Toner, W. T.; Towrie, M. *Photochem. Photobiol. Sci.* **2007**, *6*, 987−994.
(14) Chudoba, C.; Kummrow, A.; Dreyer, J.; Stenger, J.; Nibbering, E. T. J.; Elsaesser, T.; Zachariasse, K. A. *Chem. Phys. Lett.* **1999**, *309*, 357−363.
(15) Alderman, D. J. *J. Fish Dis.* **1985**, *8*, 289−298.
(16) Duxbury, D. F. *Chem. Rev.* **1993**, *93*, 381−433.
(17) Nagasawa, Y.; Ando, Y.; Kataoka, D.; Matsuda, H.; Miyasaka, H.; Okada, T. *J. Phys. Chem. A* **2002**, *106*, 2024−2035.
(18) Robla, T.; Seilmeier, A. *Chem. Phys. Lett.* **1988**, *147*, 544−550.
(19) Miyata, R.; Kimura, Y.; Terazima, M. *Chem. Phys. Lett.* **2002**, *365*, 406−412.
(20) Lian, T.; Locke, B.; Kholodenko, Y.; Hochstrasser, R. M. *J. Phys. Chem.* **1994**, *85*, 11648−11656.
(21) Vogel, M.; Rettig, W. *Ber. Bunsen-Ges. Phys. Chem.* **1985**, *89*, 962−968.
(22) Forster, T.; Hoffmann, G. *Z. Phys. Chem., Neue Folge* **1971**, *75*, 63−76.
(23) Rafiq, S.; Yadav, R.; Sen, P. *J. Phys. Chem. B* **2010**, *114*, 13988−13994.
(24) Maruyama, Y.; Magnin, O.; Satozono, H.; Ishikawa, M. *J. Phys. Chem. A* **1999**, *103*, 5629−5635.
(25) Nagasawa, Y.; Ando, Y.; Okada, T. *Chem. Phys. Lett.* **1999**, *312*, 161−168.
(26) Martin, M. M.; Plaza, P.; Changenet, P.; Meyer, Y. H. *J. Photochem. Photobiol., A* **1997**, *105*, 197−204.
(27) Li, G.; Magana, D.; Dyer, R. B. *J. Phys. Chem. B* **2012**, *116*, 3467−3475.
(28) Malkin, J. *Photophysical and Photochemical Properties of Aromatic Compounds*; CRC Press, Inc.: Boca Raton, 1992.
(29) Lee, Y. H.; Lee, M. *Bull. Korean Chem. Soc.* **1997**, *18*, 10.
(30) Yoshizawa, M.; Suzuki, K.; Kubo, A.; Saikan, S. *Chem. Phys. Lett.* **1998**, *290*, 43−48.
(31) Lueck, H. B.; Daniel, D. C.; McHale, J. L. *J. Raman Spectrosc.* **1993**, *24*, 363−370.
(32) Ayed, L.; Chaieb, K.; Cheref, A.; Bakhrouf, A. *World J. Microbiol. Biotechnol.* **2009**, *25*, 705−711.
(33) Domke, K. F.; Zhang, D.; Pettinger, B. *J. Am. Chem. Soc.* **2006**, *128*, 14721−14727.
(34) Pal, A.; Kumar, A. *J. Mol. Liq.* **2006**, *123*, 146−151.
(35) Ben-Amotz, D.; Harris, C. B. *Chem. Phys. Lett.* **1985**, *119*, 305−311.
(36) Sundström, V.; Gillbro, T. *J. Chem. Phys.* **1984**, *81*, 3463−3474.
(37) Tobita, S.; Ida, K.; Shiobara, S. *Res. Chem. Intermed.* **2001**, *27*, 205−218.
(38) Letard, J. F.; Lapouyade, R.; Rettig, W. *J. Am. Chem. Soc.* **1993**, *115*, 2441−2447.